Determination of transition matrices for inhomogeneous dielectric bodies by a wave propagator method

Karlsson, Anders

1998

CODEN:LUTEDX/(TEAT-7076)/1-17/(1998)

Determination of transition matrices for inhomogeneous dielectric bodies by a wave propagator method

Anders Karlsson

Department of Electroscience
Electromagnetic Theory
Lund Institute of Technology
Sweden

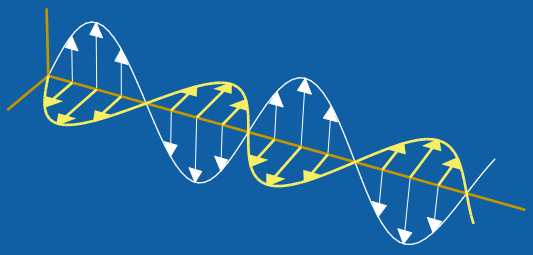

Anders Karlsson

Department of Electroscience
Electromagnetic Theory
Lund Institute of Technology
P.O. Box 118
SE-221 00 Lund
Sweden

Editor: Gerhard Kristensson

Abstract

A method for determining transition matrices for inhomogeneous dielectric shells is presented. The source can be either inside or outside the shell. The method is based upon expansions of the electric and magnetic fields in vector spherical harmonics. The expansion coefficients in the shell satisfy a system of linear ordinary differential equations in the radial direction. The expansion coefficients for the incident and scattered fields are related via transition matrices, defined in the same way as in the T-matrix or null-field method. Numerical examples show excellent agreement with results obtained by the T-matrix method. Numerically the method is particularly strong for the case of a source at the center of large, but thin, inhomogeneous spherical shell.

1 Introduction

In the present paper a method for calculating the scattered field from inhomogeneous spherical shells is presented. The source can be either outside or inside the shell. By expanding the electric and magnetic fields in vector spherical harmonics, the scattering problem is reduced to a system of first order ordinary differential equations (ODE) in the radial coordinate. Numerically these equations are straightforward to solve by some standard ODE solver. The convergence of the method depends on the variation of the permittivity in the shell, and the thickness and radius of the shell. When the source is located at the origin it is possible to determine the radiation pattern from an antenna in the center of a spherical shell for very large radii of the shell. For these type of problems the method is superior to e.g. the finite-difference-time-domain method (FDTD), the finite element method (FEM) and the method of moments (MoM), which cannot handle structures that are very large compared to the wavelength.

From the method it is easy to obtain the transition matrices for the shell, i.e. the matrices that relate the scattered field to the incident field. In particular the T-matrix that relates the scattered field to the incident field when the source is outside the shell is obtained, cf [10]. There are a number of methods and results developed for the T-matrix that then can be utilized. Thus it is possible to treat scattering from several inhomogeneous objects, [8], objects in layered structures, [7], objects in waveguides, [3], and resonances in objects, [11].

There are at least two methods that are related to the present method. One is presented in [6]. The method is based upon the integral representation of the electric field and expansion of the Green dyadics in spherical vector waves. By utilizing the invariant imbedding method a Ricatti equation is obtained for the T-matrix. The major difference between the imbedding and the propagator method is that the set of ODE:s is non-linear for the imbedding method whereas the propagator method gives a linear system of equations. Another difference is that the internal fields in the shell are easier to obtain by the propagator method. The other method is presented in [4] and [5]. In that method the Maxwell equations are rewritten in terms of the angular components of the electric and magnetic fields. By an expansion of these components in the system $\exp(i(n\cos\theta + m\phi))$ a system of ODEs is obtained.

Numerically it is expected that the two methods and the method in this paper are comparable.

The outline of the present paper is as follows: First the basic system of vector functions is defined. In Section 3 the fields are expanded in spherical harmonics in the shell and in spherical vector waves inside and outside the shell. The system of ODEs for the expansion coefficients is derived in Section 4. A wave splitting operator is defined in Section 5 where also the transition matrices are defined. The numerical algorithm and numerical examples are discussed in Section 6 for the axially symmetric shell. Energy conservation and reciprocity impose conditions on the transition matrices and this is discussed in Section 7.

2 Vector spherical harmonics and spherical vector waves

The vector spherical harmonics are defined by [2]

$$\begin{aligned}
\boldsymbol{A}_{1\sigma ml}(\hat{r}) &= \frac{1}{\sqrt{l(l+1)}}\nabla \times (\boldsymbol{r} Y_{\sigma ml}(\hat{r})) \\
\boldsymbol{A}_{2\sigma ml}(\hat{r}) &= \frac{1}{\sqrt{l(l+1)}} r\nabla Y_{\sigma ml}(\hat{r}) \\
\boldsymbol{A}_{3\sigma ml}(\hat{r}) &= \hat{r} Y_{ml}(\hat{r})
\end{aligned}$$

The following definition of the spherical harmonics is used

$$Y_{\sigma ml}(\theta,\phi) = \sqrt{\frac{\varepsilon_m}{2\pi}}\sqrt{\frac{2l+1}{2}\frac{(l-m)!}{(l+m)!}} P_l^m(\cos\theta) \begin{Bmatrix} \cos m\phi \\ \sin m\phi \end{Bmatrix}$$

where $\varepsilon_m = 2 - \delta_{m0}$ and σ, m, l take the values

$$\sigma = \begin{Bmatrix} \mathrm{e} \\ \mathrm{o} \end{Bmatrix}, \quad m = 0,\, 1,\, 2,\, \ldots,\, l, \quad l = 0,\, 1, \ldots$$

In the current application l will never have the value 0. It is convenient to introduce a multi index n for the indices σml with some convention such that $n = 1,\, 2,\, 3, \ldots$. Some of the properties of the vector spherical harmonics are

$$\begin{aligned}
&\hat{r} \cdot \boldsymbol{A}_{\tau n}(\hat{r}) = 0, \qquad \tau = 1, 2 \\
&\hat{r} \times \boldsymbol{A}_{1n}(\hat{r}) = \boldsymbol{A}_{2n}(\hat{r}) \\
&\hat{r} \times \boldsymbol{A}_{2n}(\hat{r}) = -\boldsymbol{A}_{1n}(\hat{r}) \\
&\hat{r} \times \boldsymbol{A}_{3n}(\hat{r}) = \boldsymbol{0}
\end{aligned}$$

$$\begin{aligned}
\nabla \times \boldsymbol{A}_{1n}(\hat{r}) &= \frac{1}{r}\left(\boldsymbol{A}_{2n}(\hat{r}) + \sqrt{l(l+1)}\boldsymbol{A}_{3n}(\hat{r})\right) \\
\nabla \times \boldsymbol{A}_{2n}(\hat{r}) &= -\frac{1}{r}\boldsymbol{A}_{1n}(\hat{r}) \\
\nabla \times \boldsymbol{A}_{3n}(\hat{r}) &= \frac{1}{r}\sqrt{l(l+1)}\boldsymbol{A}_{1n}(\hat{r})
\end{aligned}$$

$$\int \boldsymbol{A}_{\tau n}(\hat{r}) \cdot \boldsymbol{A}_{\tau' n'}(\hat{r}) d\Omega = \delta_{\tau\tau'}\delta_{nn'} \tag{2.1}$$

The outgoing divergence-free spherical vector waves are defined by

$$\begin{aligned}
\boldsymbol{u}_{1n}(k\boldsymbol{r}) &= h_l^{(1)}(kr)\boldsymbol{A}_{1n}(\hat{r}) \\
\boldsymbol{u}_{2n}(k\boldsymbol{r}) &= \frac{1}{k}\nabla \times \left(h_l^{(1)}(kr)\boldsymbol{A}_{1n}(\hat{r})\right)
\end{aligned}$$

The corresponding regular waves are

$$\begin{aligned}
\boldsymbol{v}_{1n}(k\boldsymbol{r}) &= j_l(kr)\boldsymbol{A}_{1n}(\hat{r}) \\
\boldsymbol{v}_{2n}(k\boldsymbol{r}) &= \frac{1}{k}\nabla \times (j_l(kr)\boldsymbol{A}_{1n}(\hat{r}))
\end{aligned}$$

3 Formulation of the problem

A spherical shell with an inner radius a and an outer radius b is located in a homogeneous medium. Without loss of generality it is assumed that there is vacuum in the two regions $r < a$ and $r > b$. The shell has an $\boldsymbol{r}$ dependent permittivity. The source is time-harmonic and is located either inside the shell, i.e. in the region $r < a_s < a$ or outside the shell, i.e. in the region $r > b_s > b$. With the time-dependence convention $e^{-i\omega t}$ the Maxwell equations in the region $b_s > r > a_s$ read

$$\begin{aligned}
\nabla \times \boldsymbol{E}(\boldsymbol{r}) &= i\omega\mu_0 \boldsymbol{H}(\boldsymbol{r}) \\
\nabla \times \boldsymbol{H}(\boldsymbol{r}) &= -i\omega\epsilon_0 \epsilon(\boldsymbol{r}) \boldsymbol{E}(\boldsymbol{r})
\end{aligned}$$

The objective is to find the scattered field in the regions $r > b_s$ and $r < a_s$, but also the internal field in the region $a_s < r < b_s$ is of interest.

4 Expansions of the fields

Consider the general case with sources in both of the regions $r < a_s$ and $r > b_s$. In the regions $r < a$ and $r > b$ the electric field is given by

$$\boldsymbol{E}(\boldsymbol{r}) = \boldsymbol{E}^{in}(\boldsymbol{r}) + \boldsymbol{E}^{r}(\boldsymbol{r}) \qquad \text{when } r < a \tag{4.1}$$

$$\boldsymbol{E}(\boldsymbol{r}) = \boldsymbol{E}^{out}(\boldsymbol{r}) + \boldsymbol{E}^{s}(\boldsymbol{r}) \qquad \text{when } r > b \tag{4.2}$$

where $\boldsymbol{E}^{in}(\boldsymbol{r})$ is the field in free space from the source in $r < a_s$ and $\boldsymbol{E}^{out}(\boldsymbol{r})$ is the field in free space from the source in $r > b_s$. The fields in Eqs. (4.1) and (4.2) are expanded in spherical vector waves with the condition that $\boldsymbol{E}^{out}(\boldsymbol{r})$ and $\boldsymbol{E}^{r}(\boldsymbol{r})$ are regular in $r < b_s$ and $r < a$, respectively. The field $\boldsymbol{E}^{in}(\boldsymbol{r})$ is the field from the source in $r < a_s$ in free space, and thus $\boldsymbol{E}^{in}(\boldsymbol{r})$ and $\boldsymbol{E}^{s}(\boldsymbol{r})$ satisfy radiation conditions for

large r

$$\begin{aligned}
\boldsymbol{E}^{in}(\boldsymbol{r}) &= \sum_{\tau=1}^{2}\sum_{n} a_{\tau n}^{in}\boldsymbol{u}_{\tau n} \\
&= \sum_{\tau=1}^{2}\sum_{l=1}^{\infty}\sum_{m=0}^{l}\sum_{\sigma=e,0} a_{\tau\sigma ml}^{in}\boldsymbol{u}_{\tau\sigma ml}(k_0\boldsymbol{r}), \qquad \text{when } a_s < r < a \qquad (4.3)\\
\boldsymbol{E}^{out}(\boldsymbol{r}) &= \sum_{\tau=1}^{2}\sum_{n} a_{\tau n}^{out}\boldsymbol{v}_{\tau n}, \qquad \text{when } b < r < b_s \qquad (4.4)\\
\boldsymbol{E}^{r}(\boldsymbol{r}) &= \sum_{\tau=1}^{2}\sum_{n} b_{\tau n}\boldsymbol{v}_{\tau n}, \qquad \text{when } r < a \qquad (4.5)\\
\boldsymbol{E}^{s}(\boldsymbol{r}) &= \sum_{\tau=1}^{2}\sum_{n} f_{\tau n}\boldsymbol{u}_{\tau n}, \qquad \text{when } r > b \qquad (4.6)
\end{aligned}$$

The coefficients $a_{\tau n}^{in}$ and $a_{\tau n}^{out}$ are assumed to be known. The scattering problem is to determine the coefficients $b_{\tau n}$ and $f_{\tau n}$ and, if needed, the internal fields in the shell.

In the shell, $a < r < b$, the spherical vector waves do not satisfy the Maxwell equations. Instead an expansion in vector spherical harmonics are used where the r-dependent expansion coefficients satisfy a system of ordinary differential equations (ODE). The electric field is not divergence free in the shell and a general expansion in vector spherical harmonics reads

$$\begin{aligned}
\boldsymbol{E}(\boldsymbol{r}) &= \sum_{n}\frac{e_{1n}(k_0r)}{k_0r}\boldsymbol{A}_{1n}(\hat{r}) + \nabla\times\left(\frac{e_{2n}(k_0r)}{k_0^2r}\boldsymbol{A}_{1n}(\hat{r})\right) + \frac{e_{3n}(k_0r)}{k_0r}\boldsymbol{A}_{3n}(\hat{r}) \\
&= \sum_{n}\frac{e_{1n}(k_0r)}{k_0r}\boldsymbol{A}_{1n}(\hat{r}) + \frac{e'_{2n}(k_0r)}{k_0r}\boldsymbol{A}_{2n}(\hat{r}) \qquad (4.7)\\
&\quad + \left(\frac{e_{2n}(k_0r)}{k_0^2r^2}\sqrt{l(l+1)} + \frac{e_{3n}(k_0r)}{k_0r}\right)\boldsymbol{A}_{3n}(\hat{r}), \qquad a < r < b
\end{aligned}$$

where prime denotes differentiation with respect to the argument k_0r. The magnetic field is divergence free and is expanded as

$$\begin{aligned}
i\eta_0\boldsymbol{H}(\boldsymbol{r}) &= \sum_{n}\frac{h_{1n}(k_0r)}{k_0r}\boldsymbol{A}_{1n}(\hat{r}) + \nabla\times\left(\frac{h_{2n}(k_0r)}{k_0^2r}\boldsymbol{A}_{1n}(\hat{r})\right) \\
&= \sum_{n}\frac{h_{1n}(k_0r)}{k_0r}\boldsymbol{A}_{1n}(\hat{r}) + \frac{h'_{2n}(k_0r)}{k_0r}\boldsymbol{A}_{2n}(\hat{r}) \qquad (4.8)\\
&\quad + \frac{h_{2n}(k_0r)}{k_0^2r^2}\sqrt{l(l+1)}\boldsymbol{A}_{3n}(\hat{r}), \qquad a < r < b
\end{aligned}$$

The expansions (4.7) and (4.8) are inserted into the induction law $\nabla\times\boldsymbol{E}(\boldsymbol{r}) =$

$i\omega\mu_0 \boldsymbol{H}(\boldsymbol{r})$ where

$$\begin{aligned}\nabla \times \boldsymbol{E}(\boldsymbol{r}) =& \sum_n \frac{1}{r}\left(\frac{e_{3n}(k_0 r)}{k_0 r}\sqrt{l(l+1)} - e''_{2n}(k_0 r) + l(l+1)\frac{e_{2n}(k_0 r)}{k_0^2 r^2}\right)\boldsymbol{A}_{1n}(\hat{r}) \\ &+ \frac{e'_{1n}(k_0 r)}{k_r}\boldsymbol{A}_{2n}(\hat{r}) + \frac{e_{1n}(k_0 r)}{k_0 r^2}\sqrt{l(l+1)}\boldsymbol{A}_{3n}(\hat{r})\end{aligned}$$

The orthogonality of the vector spherical harmonics in Eq. (2.1) gives

$$h_{2n}(k_0 r) = e_{1n}(k_0 r) \tag{4.9}$$

$$h_{1n}(k_0 r) = \frac{e_{3n}(k_0 r)}{k_0 r}\sqrt{l(l+1)} - e''_{2n}(k_0 r) + l(l+1)\frac{e_{2n}(k_0 r)}{k_0^2 r^2} \tag{4.10}$$

Ampère's law, $\nabla \times \boldsymbol{H}(\boldsymbol{r}) = -i\omega\epsilon_0\epsilon(\boldsymbol{r})\boldsymbol{E}(\boldsymbol{r})$ gives

$$\begin{aligned}&\sum_n \frac{1}{r}\left(\frac{h_{2n}(k_0 r)}{k_0^2 r^2}l(l+1) - h''_{2n}(k_0 r)\right)\boldsymbol{A}_{1n}(\hat{r}) \\ &\qquad + \frac{h'_{1n}(k_0 r)}{r}\boldsymbol{A}_{2n}(\hat{r}) + \frac{h_{1n}(k_0 r)}{k_0 r^2}\sqrt{l(l+1)}\boldsymbol{A}_{3n}(\hat{r}) \\ &\quad = \frac{k^2(\boldsymbol{r})}{k_0}\sum_n \frac{e_{1n}(k_0 r)}{k_0 r}\boldsymbol{A}_{1n}(\hat{r}) + \frac{e'_{2n}(k_0 r)}{k_0 r}\boldsymbol{A}_{2n}(\hat{r}) \\ &\qquad + \left(\sqrt{l(l+1)}\frac{e_{2n}(k_0 r)}{k_0^2 r^2} + \frac{e_{3n}(k_0 r)}{k_0 r}\right)\boldsymbol{A}_{3n}(\hat{r})\end{aligned}$$

Orthogonality gives

$$\begin{aligned}h''_{2n}(k_0 r) - l(l+1)\frac{h_{2n}(r)}{k_0^2 r^2} =& -\sum_{n'} h_{2n'}(k_0 r)\int_\Omega \frac{k^2(\boldsymbol{r})}{k_0^2}\boldsymbol{A}_{1n'}(\hat{r})\cdot\boldsymbol{A}_{1n}(\hat{r})d\Omega \\ &+ e'_{2n'}(k_0 r)\int \frac{k^2(\boldsymbol{r})}{k_0^2}\boldsymbol{A}_{2n'}(\hat{r})\cdot\boldsymbol{A}_{1n}(\hat{r})d\Omega\end{aligned} \tag{4.11}$$

$$\begin{aligned}h'_{1n}(k_0 r) =& \sum_{n'} h_{2n'}(k_0 r)\int_\Omega \frac{k^2(\boldsymbol{r})}{k_0^2}\boldsymbol{A}_{1n'}(\hat{r})\cdot\boldsymbol{A}_{2n}(\hat{r})d\Omega \\ &+ e'_{2n'}(k_0 r)\int_\Omega \frac{k^2(\boldsymbol{r})}{k_0^2}\boldsymbol{A}_{2n'}(\hat{r})\cdot\boldsymbol{A}_{2n}(\hat{r})d\Omega\end{aligned} \tag{4.12}$$

$$\begin{aligned}e''_{2n}(k_0 r) + h_{1n}(k_0 r) =& \sqrt{l(l+1)} \\ &\sum_{n'} h_{1n'}(k_0 r)\sqrt{l'(l'+1)}\int \frac{1}{k^2(\boldsymbol{r})r^2}\boldsymbol{A}_{3n'}(\hat{r})\cdot\boldsymbol{A}_{3n}(\hat{r})d\Omega\end{aligned} \tag{4.13}$$

The functions $h_{1n}(r)$, $h_{2n}(r)$, $h'_{2n}(r)$, $e'_{2n}(r)$ are all continuous functions and satisfy Eqs. (4.9)–(4.13), that are equivalent to the first order system of ODE

$$\frac{\partial}{\partial k_0 r}\begin{pmatrix} h_{2n}(k_0r) \\ h'_{2n}(k_0r) \\ h_{1n}(k_0r) \\ e'_{2n}(k_0r) \end{pmatrix} = D_n \begin{pmatrix} h_{2n}(k_0r) \\ h'_{2n}(k_0r) \\ h_{1n}(k_0r) \\ e'_{2n}(k_0r) \end{pmatrix} + \sum_{n'} C_{n,n'} \begin{pmatrix} h_{2n'}(k_0r) \\ h'_{2n'}(k_0r) \\ h_{1n'}(k_0r) \\ e'_{2n'}(k_0r) \end{pmatrix} \tag{4.14}$$

The blocks $C_{n,n'}$ and D_n are given by

$$C_{n,n'} = \begin{pmatrix} 0 & 0 & 0 & 0 \\ \alpha^{21}_{n,n'} & 0 & 0 & \alpha^{24}_{n,n'} \\ \alpha^{31}_{n,n'} & 0 & 0 & \alpha^{34}_{n,n'} \\ 0 & 0 & \alpha^{43}_{n,n'} & 0 \end{pmatrix}$$

$$D_n = \begin{pmatrix} 0 & 1 & 0 & 0 \\ \frac{l(l+1)}{k_0^2 r^2} - 1 & 0 & 0 & 0 \\ 0 & 0 & 0 & 1 \\ 0 & 0 & \frac{l(l+1)}{k_0^2 r^2} - 1 & 0 \end{pmatrix}$$

The coefficients α read

$$\alpha^{21}_{n,n'} = -\int \left(\frac{k^2(\boldsymbol{r})}{k_0^2} - 1 \right) \boldsymbol{A}_{1n}(\hat{r}) \cdot \boldsymbol{A}_{1n'}(\hat{r}) d\Omega$$

$$\alpha^{24}_{n,n'} = -\int \frac{k^2(\boldsymbol{r})}{k_0^2} \boldsymbol{A}_{1n}(\hat{r}) \cdot \boldsymbol{A}_{2n'}(\hat{r}) d\Omega = -\int \left(\frac{k^2(\boldsymbol{r})}{k_0^2} - 1 \right) \boldsymbol{A}_{1n}(\hat{r}) \cdot \boldsymbol{A}_{2n'}(\hat{r}) d\Omega$$

$$\alpha^{31}_{n,n'} = \int \frac{k^2(\boldsymbol{r})}{k_0^2} \boldsymbol{A}_{2n}(\hat{r}) \cdot \boldsymbol{A}_{1n'}(\hat{r}) d\Omega = \int \left(\frac{k^2(\boldsymbol{r})}{k_0^2} - 1 \right) \boldsymbol{A}_{2n}(\hat{r}) \cdot \boldsymbol{A}_{1n'}(\hat{r}) d\Omega$$

$$\alpha^{34}_{n,n'} = \int \left(\frac{k^2(\boldsymbol{r})}{k_0^2} - 1 \right) \boldsymbol{A}_{2n}(\hat{r}) \cdot \boldsymbol{A}_{2n'}(\hat{r}) d\Omega$$

$$\alpha^{43}_{n,n'} = \frac{1}{k_0^2 r^2} \sqrt{l(l+1)} \sqrt{l'(l'+1)} \int \left(\frac{k_0^2}{k^2(\boldsymbol{r})} - 1 \right) \boldsymbol{A}_{3n}(\hat{r}) \cdot \boldsymbol{A}_{3n'}(\hat{r}) d\Omega$$

The propagator matrix $K(r, r')$ is a matrix-valued mapping that is independent of the fields. It is defined as

$$\begin{pmatrix} h_{2n}(k_0r) \\ h'_{2n}(k_0r) \\ h_{1n}(k_0r) \\ e'_{2n}(k_0r) \end{pmatrix} = \sum_{n'} K_{n,n'}(r, r') \begin{pmatrix} h_{2n'}(k_0r') \\ h'_{2n'}(k_0r') \\ h_{1n'}(k_0r') \\ e'_{2n'}(k_0r') \end{pmatrix} \tag{4.15}$$

where

$$K_{n,n'}(r, r') = \begin{pmatrix} K^{11}_{n,n'} & K^{12}_{n,n'} & K^{13}_{n,n'} & K^{14}_{n,n'} \\ K^{21}_{n,n'} & K^{22}_{n,n'} & K^{23}_{n,n'} & K^{24}_{n,n'} \\ K^{31}_{n,n'} & K^{32}_{n,n'} & K^{33}_{n,n'} & K^{34}_{n,n'} \\ K^{41}_{n,n'} & K^{42}_{n,n'} & K^{43}_{n,n'} & K^{44}_{n,n'} \end{pmatrix}$$

By inserting the definition (4.15) into Eq. (4.14) it is seen that $K_{n,n'}(r,r')$ satisfies the ODE

$$\begin{aligned}\frac{\partial K_{n,n'}(r,r')}{\partial k_0 r} &= D_n K_{n,n'}(r,r') + \sum_{n''} C_{n,n''} K_{n'',n'}(r,r') \\ K_{n,n'}(r',r') &= \delta_{nn'} \begin{pmatrix} 1 & 0 & 0 & 0 \\ 0 & 1 & 0 & 0 \\ 0 & 0 & 1 & 0 \\ 0 & 0 & 0 & 1 \end{pmatrix}\end{aligned} \tag{4.16}$$

The following useful relations are easy to obtain from Eq. (4.15)

$$\begin{aligned}K(r,r')K(r',r'') &= K(r,r'') \\ K^{-1}(r,r') &= K(r',r)\end{aligned}$$

Notice that K is a real matrix when the shell is lossless since C and D then are real.

5 Wave splitting and transition matrices

At the boundaries, $r = a$ and $r = b$, the fields in the expansions (4.7) and (4.8) have to be related to those in the expansions (4.3)–(4.6). This relation is expressed in terms of the splitting matrix, P, that splits the field into an outward moving part and a regular part. In vacuum the system of equations (4.14) are for every n divided into two systems, each containing two equations

$$\begin{aligned}\frac{\partial}{\partial k_0 r}\begin{pmatrix} h_{2n}(k_0 r) \\ h'_{2n}(k_0 r)\end{pmatrix} &= \begin{pmatrix} 0 & 1 \\ \frac{l(l+1)}{k_0^2 r^2} - 1 & 0\end{pmatrix}\begin{pmatrix} h_{2n}(k_0 r) \\ h'_{2n}(k_0 r)\end{pmatrix} = d_n \begin{pmatrix} h_{2n}(k_0 r) \\ h'_{2n}(k_0 r)\end{pmatrix} \\ \frac{\partial}{\partial k_0 r}\begin{pmatrix} h_{1n}(k_0 r) \\ e'_{2n}(k_0 r)\end{pmatrix} &= \begin{pmatrix} 0 & 1 \\ \frac{l(l+1)}{k_0^2 r^2} - 1 & 0\end{pmatrix}\begin{pmatrix} h_{1n}(k_0 r) \\ e'_{2n}(k_0 r)\end{pmatrix} = d_n \begin{pmatrix} h_{1n}(k_0 r) \\ e'_{2n}(k_0 r)\end{pmatrix}\end{aligned}$$

Now define the functions

$$\begin{aligned}\Gamma_l(k_0 r) &= k_0 r h_l^{(1)}(k_0 r) e^{-ik_0 r} \\ \gamma_l(k_0 r) &= k_0 r j_l(k_0 r) e^{ik_0 r}\end{aligned}$$

where $j_l(k_0 r)$ is the spherical Bessel function of order l and $h_l^{(1)}(k_0 r)$ is the spherical Hankel function of the first kind. The functions Γ_l and γ_l satisfy the equations

$$\begin{aligned}\Gamma_l''(k_0 r) + 2i\Gamma_l'(k_0 r) - \frac{l(l+1)}{k_0^2 r^2}\Gamma_l(k_0 r) = 0 \\ \gamma_l''(k_0 r) - 2i\gamma_l'(k_0 r) - \frac{l(l+1)}{k_0^2 r^2}\gamma_l(k_0 r) = 0\end{aligned}$$

Introduce the following transformation:

$$\begin{pmatrix} h_{2n} \\ h'_{2n}\end{pmatrix} = \begin{pmatrix} \Gamma_l & \gamma_l \\ \Gamma_l' + i\Gamma_l & \gamma_l' - i\gamma_l\end{pmatrix}\begin{pmatrix} v_{1n}^+(r) \\ v_{1n}^-(r)\end{pmatrix} = p_n^{-1}\begin{pmatrix} v_{1n}^+(r) \\ v_{1n}^-(r)\end{pmatrix} \tag{5.1}$$

and

$$\begin{pmatrix} h_{1n} \\ e'_{2n} \end{pmatrix} = \begin{pmatrix} \Gamma_l & \gamma_l \\ \Gamma'_l + i\Gamma_l & \gamma'_l - i\gamma_l \end{pmatrix} \begin{pmatrix} v^+_{2n}(r) \\ v^-_{2n}(r) \end{pmatrix} = p_n^{-1} \begin{pmatrix} v^+_{2n}(r) \\ v^-_{2n}(r) \end{pmatrix} \tag{5.2}$$

In vacuum this transformation is a wave splitting that decomposes the field into outward and inward moving fields. Since v^+ is related to to far-field the transformation is denoted the far-field to total field transformation.

The total field to far-field transformation is obtained from the Wronskian for the Hankel and Bessel functions that implies

$$i\Gamma_l\gamma'_l - i\gamma_l\Gamma'_l + 2\Gamma_l\gamma_l = 1 \tag{5.3}$$

Using the Wronskian in Eq. (5.3), the total field to far-field transformation is obtained as

$$\begin{pmatrix} v^+_{1n} \\ v^-_{1n} \end{pmatrix} = \begin{pmatrix} \gamma_l + i\gamma'_l & -i\gamma_l \\ \Gamma_l - i\Gamma'_l & i\Gamma_l \end{pmatrix} \begin{pmatrix} h_{2n} \\ h'_{2n} \end{pmatrix} = p_n \begin{pmatrix} h_{2n} \\ h'_{2n} \end{pmatrix} \tag{5.4}$$

and

$$\begin{pmatrix} v^+_{2n} \\ v^-_{2n} \end{pmatrix} = p_n \begin{pmatrix} h_{1n} \\ e'_{2n} \end{pmatrix} \tag{5.5}$$

In vacuum the split fields satisfy the diagonal system of ODEs

$$\frac{\partial}{\partial k_0 r} \begin{pmatrix} v^+_{\tau n} \\ v^-_{\tau n} \end{pmatrix} = (p_n d_n p_n^{-1} - p_n \frac{\partial p_n^{-1}}{\partial k_0 r}) \begin{pmatrix} v^+_{\tau n} \\ v^-_{\tau n} \end{pmatrix} = i \begin{pmatrix} 1 & 0 \\ 0 & -1 \end{pmatrix} \begin{pmatrix} v^+_{\tau n} \\ v^-_{\tau n} \end{pmatrix}$$

with solutions $v^\pm_{\tau n}(r) = V^\pm_{\tau n} e^{\pm ikr}$. In the region $r > b_s$ the constants $V^+_{\tau n}$ are the far-field amplitudes of the scattered field. It is possible to obtain the equation for the split fields $v^\pm$ also in the shell, and one can introduce propagators for the split fields. These propagators are seen to satisfy the same equations as $v^\pm$ and these equations can be used instead of Eq. (4.16). However, the system (4.16) is simpler and gives a somewhat faster numerical algorithm.

The relation between the expansion coefficients in Eqs. (4.3)–(4.6) and the split fields $v^\pm_\tau$ follows from Eqs. (5.4) and (5.5)

$$\begin{aligned} a^{in}_{\tau\sigma ml} &= v^+_{\tau\sigma ml}(a)e^{-ik_0 a} \\ a^{out}_{\tau\sigma ml} &= v^-_{\tau\sigma ml}(b)e^{ik_0 b} \\ b_{\tau\sigma ml} &= v^-_{\tau\sigma ml}(a)e^{ik_0 a} \\ f_{\tau\sigma ml} &= v^+_{\tau\sigma ml}(b)e^{-ik_0 b} \end{aligned} \tag{5.6}$$

The transition matrices are defined by

$$\begin{aligned} \begin{pmatrix} f_{1n} \\ f_{2n} \end{pmatrix} &= \sum_{n'} T_{n,n'} \begin{pmatrix} a^{out}_{1n'} \\ a^{out}_{2n'} \end{pmatrix} + Q^{-1}_{n,n'} \begin{pmatrix} a^{in}_{1n'} \\ a^{in}_{2n'} \end{pmatrix} \\ \begin{pmatrix} b_{1n} \\ b_{2n} \end{pmatrix} &= \sum_{n'} \tilde{Q}^{-1}_{n,n'} \begin{pmatrix} a^{out}_{1n} \\ a^{out}_{2n} \end{pmatrix} + R_{n,n'} \begin{pmatrix} a^{in}_{1n} \\ a^{in}_{2n} \end{pmatrix} \end{aligned} \tag{5.7}$$

The matrices Q, $\tilde{Q}$, R and T have the 2×2 block structure

$$Q_{n,n'} = \begin{pmatrix} Q^{11}_{n,n'} & Q^{12}_{n,n'} \\ Q^{21}_{n,n'} & Q^{22}_{n,n'} \end{pmatrix}$$

Let

$$P(r) = \begin{pmatrix} P_1(r) & 0 & 0 & \cdots \\ 0 & P_2(r) & 0 & \cdots \\ 0 & 0 & P_3(r) & \cdots \\ \vdots & \vdots & \vdots & \end{pmatrix}$$

where

$$P_n(r) = \begin{pmatrix} p_n(r) & 0 \\ 0 & p_n(r) \end{pmatrix}$$

It is then seen from Eqs. (5.1), (5.2), (5.6) and (4.15) that

$$\begin{aligned} Q^{ij}_{n,n'} &= \big(P(a)K(a,b)P^{-1}(b)\big)^{2i-1,2j-1}_{n,n'}\, e^{ik_0(b-a)} \\ \tilde{Q}^{ij}_{n,n'} &= \big(P(b)K(b,a)P^{-1}(a)\big)^{2i,2j}_{n,n'}\, e^{ik_0(b-a)} \end{aligned} \quad , \quad i = 1,2,\ j = 1,2$$

The matrices R and T can be written as

$$\begin{aligned} R &= -\tilde{Q}^{-1}\tilde{M} \\ T &= -Q^{-1}M \end{aligned}$$

where

$$\begin{aligned} \tilde{M}^{ij}_{n,n'} &= \big(P(b)K(b,a)P^{-1}(a)\big)^{2i,2j-1}_{n,n'}\, e^{-ik_0(a+b)} \\ M^{ij}_{n,n'} &= \big(P(a)K(a,b)P^{-1}(b)\big)^{2i-1,2j}_{n,n'}\, e^{ik_0(a+b)} \end{aligned} \quad , \quad i = 1,2,\ j = 1,2$$

6 A numerical algorithm and numerical examples

Equation (4.16) can be solved by an ODE solver. A simple type of ODE solver is based upon the trapezoidal rule and gives the following scheme

$$\begin{aligned} K(a+p\Delta r, a) = &\left[I - \frac{\Delta r}{2}(D(a+p\Delta r) + C(a+p\Delta r)\right]^{-1} \\ &\left[I + \frac{\Delta r}{2}(D(a+(p-1)\Delta r) + C(a+(p-1)\Delta r)\right] K(a+(p-1)\Delta r, a) \end{aligned} \tag{6.1}$$

where Δr is the grid size. The boundary value for K is

$$K_{n,n'}(a,a) = \delta_{nn'} \begin{pmatrix} 1 & 0 & 0 & 0 \\ 0 & 1 & 0 & 0 \\ 0 & 0 & 1 & 0 \\ 0 & 0 & 0 & 1 \end{pmatrix}$$

Of course there are a number of other ODE solvers that can be used. Numerically the trapezoidal rule and a third order Runge-Kutta method give the same accuracy. For large systems Runge-Kutta methods might be faster since they do not include matrix inversions.

In the numerical examples only the axially symmetric case $\epsilon(\boldsymbol{r}) = \epsilon(r,\theta)$ is considered. All matrices then become diagonal in the indices m and σ, and every $m-$value can be treated separately. The following integrals appear in the α coefficients when there is no ϕ-dependence in $\epsilon(\boldsymbol{r})$:

$$
\begin{aligned}
I_{1n,1n'}(r,\theta) &= \int_0^{2\pi} \boldsymbol{A}_{1n}(\hat{r})\cdot\boldsymbol{A}_{1n'}(\hat{r})d\phi = \int_0^{2\pi} \boldsymbol{A}_{2n}(\hat{r})\cdot\boldsymbol{A}_{2n'}(\hat{r})d\phi \\
&= \delta_{\sigma\sigma'}\delta_{mm'}\eta_{mll'}\left(\frac{\partial P_l^m(\cos\theta)}{\partial\theta}\frac{\partial P_{l'}^m(\cos\theta)}{\partial\theta} + \frac{m^2}{\sin^2\theta}P_l^m(\cos\theta)P_{l'}^m(\cos\theta)\right) \\
I_{1n,2n'}(r,\theta) &= \int_0^{2\pi} \boldsymbol{A}_{1n}(\hat{r})\cdot\boldsymbol{A}_{2n'}(\hat{r})d\phi = -\int_0^{2\pi} \boldsymbol{A}_{2n}(\hat{r})\cdot\boldsymbol{A}_{1n'}(\hat{r})d\phi \\
&= (\delta_{\sigma o}\delta_{\sigma' e} - \delta_{\sigma e}\delta_{\sigma' o})\delta_{mm'}m\eta_{mll'}\frac{1}{\sin\theta}\left(P_l^m(\cos\theta)\frac{\partial P_{l'}^m(\cos\theta)}{\partial\theta} + P_{l'}^m(\cos\theta)\frac{\partial P_l^m(\cos\theta)}{\partial\theta}\right) \\
I_{3n,3n'}(r,\theta) &= \sqrt{l(l+1)}\sqrt{l'(l'+1)}\int_0^{2\pi} \boldsymbol{A}_{3n}(\hat{r})\cdot\boldsymbol{A}_{3n'}(\hat{r})d\phi \\
&= \delta_{\sigma\sigma'}\delta_{mm'}l(l+1)l'(l'+1)\eta_{mll'}P_l^m(\cos\theta)P_{l'}^m(\cos\theta)
\end{aligned}
$$

where

$$
\eta_{mll'} = \sqrt{\frac{2l+1}{2l(l+1)}\frac{(l-m)!}{(l+m)!}}\sqrt{\frac{2l'+1}{2l'(l'+1)}\frac{(l'-m)!}{(l'+m)!}}
$$

The α coefficients then read

$$
\begin{aligned}
\alpha_{n,n'}^{21}(r) &= -\alpha_{n,n'}^{34}(r) = -\int_0^{\pi}(\epsilon(r,\theta)-1)I_{1n,1n'}(r,\theta)\sin\theta\,d\theta \\
\alpha_{n,n'}^{24}(r) &= \alpha_{n,n'}^{31}(r) = -\int_0^{\pi}(\epsilon(r,\theta)-1)I_{1n,2n'}(r,\theta)\sin\theta\,d\theta \\
\alpha_{n,n'}^{43}(r) &= \frac{1}{k_0^2r^2}\int_0^{\pi}\left(\frac{1}{\epsilon(r,\theta)}-1\right)I_{3n,3n'}(r,\theta)\sin\theta\,d\theta
\end{aligned}
\tag{6.2}
$$

The $K-$matrix now decouples into two matrices. If the indices $ml, m'l'$ are suppressed the structure of the K-matrix is

$$
K_{\sigma,\sigma'}(r,r') = \begin{pmatrix}
K_{\mathrm{e,e}}^{11} & K_{\mathrm{e,e}}^{12} & K_{\mathrm{e,o}}^{13} & K_{\mathrm{e,o}}^{14} \\
K_{\mathrm{e,e}}^{21} & K_{\mathrm{e,e}}^{22} & K_{\mathrm{e,o}}^{23} & K_{\mathrm{e,o}}^{24} \\
K_{\mathrm{o,e}}^{31} & K_{\mathrm{o,e}}^{32} & K_{\mathrm{o,o}}^{33} & K_{\mathrm{o,o}}^{34} \\
K_{\mathrm{o,e}}^{41} & K_{\mathrm{o,e}}^{42} & K_{\mathrm{o,o}}^{43} & K_{\mathrm{o,o}}^{44}
\end{pmatrix}
$$

The other decoupled equation is found by exchanging $\sigma = \mathrm{e}$ and $\sigma = \mathrm{o}$ everywhere.

6.1 Electric dipole excitation

The simplest example of an axially symmetric source is an electric dipole $\boldsymbol{p} = p\hat{z}$ at the origin. When $p = 1$, the corresponding magnetic and electric fields are given by

$$\boldsymbol{H}^{in}(\boldsymbol{r}) = -\frac{i}{\sqrt{6\pi}}\omega k^2 h_1^{(1)}(kr)\boldsymbol{A}_{1\mathrm{e}01}(\hat{r}) = -\frac{i}{\sqrt{6\pi}}\omega k^2 \boldsymbol{u}_{1\mathrm{e}01}(\boldsymbol{r})$$
$$\boldsymbol{E}^{in}(\boldsymbol{r}) = \frac{i}{\omega\epsilon_0}\nabla \times \boldsymbol{H}(\boldsymbol{r}) = \frac{k^3}{\sqrt{6\pi\epsilon_0}}\boldsymbol{u}_{2\mathrm{e}01}(\boldsymbol{r})$$

Thus

$$a_{\tau\sigma ml} = \frac{k^3}{\sqrt{6\pi\epsilon_0}}\delta_{\tau 2}\delta_{\sigma\mathrm{e}}\delta_{m0}\delta_{l1}$$

and the transmitted field in the region $r > b$ from a dipole at the origin reads

$$\boldsymbol{E}^s(\boldsymbol{r}) = \sum_{l=1}^{\infty} f_{2\mathrm{e}0l}\boldsymbol{u}_{2\mathrm{e}0l}(\boldsymbol{r})$$

where, from Eq. (5.7)

$$f_{2\mathrm{e}0l} = Q^{-1}_{2\mathrm{e}0l,2\mathrm{e}01}a_{2\mathrm{e}01}$$

Since $h_l^{(1)}(kr) \to i^{-l-1}e^{ikr}/kr$ when $kr \to \infty$ the radiation pattern from the dipole is given by

$$\begin{aligned}|\boldsymbol{F}(\boldsymbol{r})| &= |\sum_{l=1}^{\infty} i^{-l}\boldsymbol{A}_{2\mathrm{e}0l}(\hat{r})Q^{-1}_{2\mathrm{e}0l,2\mathrm{e}01}a_{2\mathrm{e}01}| \\ &= |\sum_{l=1}^{\infty}\frac{k^3}{2\pi\epsilon_0}\sqrt{\frac{2l+1}{6l(l+1)}}\sin\theta P_l'(\cos\theta)i^{-l}Q^{-1}_{2e0l,2e01}|\end{aligned}$$

where the far field amplitude $\boldsymbol{F}$ is defined by

$$\boldsymbol{E}^s(\boldsymbol{r}) = \boldsymbol{F}(\hat{r})\frac{e^{ikr}}{kr}, \qquad \text{when } r \to \infty$$

In Figs 1 and 2 the radiation pattern from a dipole in two different thin spherical shells are presented. The thickness of the shell is $kd = 0.5$ and the inner radius is $ka = 300$ in Fig. 1 and $ka = 301.5$ in Fig. 2. The permittivity of both shells is $\epsilon = 2 + \cos 100\theta$. It turns out that it is sufficient to use truncation $l_{max} = 104$ both cases in order for the method to converge. It is clear that a truncation less than 100 in the two examples would give erroneous results since ϵ can be expanded in a series of Legendre functions with a maximum $l-$value 100. The coupling to

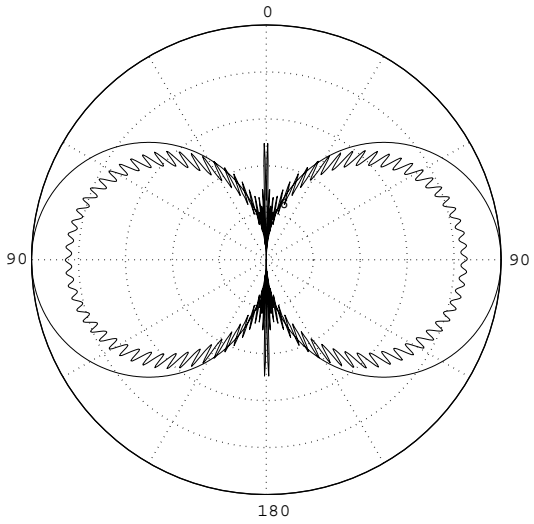

Figure 1: The radiation pattern from an electric dipole, $\boldsymbol{p} = p\hat{z}$, in a spherical shell with inner radius $ka = 300$, outer radius $kb = 300.5$ and permittivity $\epsilon = 2+\cos 100\theta$, compared to the radiation pattern for a dipole in vacuum. The truncation is $l_{\max} = 104$. Equation (4.14) was solved by the trapezoidal rule with 64 points, and the integrals in Eq. (6.2) were solved by the trapezoidal rule with 256 points.

$l-$values higher than 102 is very weak. A source with a more narrow main lobe is expected to require higher truncation. It is interesting to notice that the radius of the sphere does not affect the truncation or the number of integration points. One can easily do the same numerical calculations for a sphere with any radius. There is a considerable difference in the radiation pattern in the two figures 1 and 2. The reason is that the difference in radius of the shell between the two figures is a quarter of a wavelength. There is then destructive interference in Fig. 1 and constructive interference in Fig. 2 between the wave that is reflected once from the shell and the wave that has traveled directly from the source. There is radiation in the direction $\theta = 0$ and 180 degrees, even though the dipole in free space has no radiation in these directions. There seems to be some kind of surface wave that gives rise to this radiation.

6.2 An incident plane wave

Consider a plane wave incident along the direction $\hat{k} = \sin\theta_i\hat{x} + \cos\theta_i\hat{z}$ with the following polarization

$$\boldsymbol{E}^{out}(\boldsymbol{r}) = -E_0\frac{i}{4\pi}e^{ik_0(\sin\theta_i x+\cos\theta_i z)}\hat{y}$$

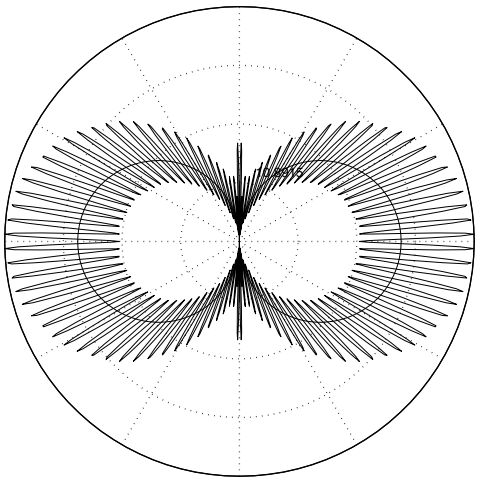

Figure 2: The radiation pattern for an electric dipole, $\boldsymbol{p} = p\hat{z}$, in a spherical shell with inner radius $ka = 301.5$, outer radius $kb = 302$ and permittivity $\epsilon = 2+\cos 100\theta$, compared to the radiation pattern for a dipole in vacuum. The truncation of the matrices is $l_{\max} = 104$. Equation (4.14) was solved by the trapezoidal rule with 64 points and the integrals in Eq. (6.2) were solved by the trapezoidal rule with 256 points. The radius of the shell is here quarter of a wavelength larger than in Fig. 1

The expansion of the plane wave in regular spherical vector wave can be found in [9] and [2]. Thus

$$\begin{aligned} a_{\tau\sigma ml} =& E_0 i^l \sqrt{\frac{\varepsilon_m}{2\pi}\frac{2l+1}{2l(l+1)}\frac{(l-m)!}{(l+m)!}} \\ & \left(-\delta_{\tau 1}\delta_{\sigma \mathrm{e}} i \sin\theta_i P_l^{m\prime}(\cos\theta_i) - \delta_{\tau 2}\delta_{\sigma \mathrm{o}}\frac{m}{\sin\theta_i}P_l^m(\cos\theta_i)\right) \end{aligned}$$

The scattered field is given by

$$\boldsymbol{E}^s(\boldsymbol{r}) = \sum_{ml} f_{1eml}\boldsymbol{u}_{1eml} + f_{2oml}\boldsymbol{u}_{2oml}$$

where

$$\begin{pmatrix} f_{1eml} \\ f_{2oml} \end{pmatrix} = \sum_{m'l'} \begin{pmatrix} T_{1eml,1em'l'}a_{1em'l'} + T_{1eml,2om'l'}a_{2om'l'} \\ T_{2oml,1em'l'}a_{1em'l'} + T_{2oml,2om'l'}a_{2om'l'} \end{pmatrix}$$

In Fig. 3 the normalized differential scattering cross section for a plane wave that impinges on a prolate spheroid is presented. The normalized differential scattering cross section is defined as in Ref. [1] by

$$\frac{\sigma_d(\theta,\phi)}{\pi b^2} = \frac{|\boldsymbol{F}(\theta,\phi)|^2}{\pi b^2}$$

where b is the radius of the smallest sphere that circumscribes the scatterer.

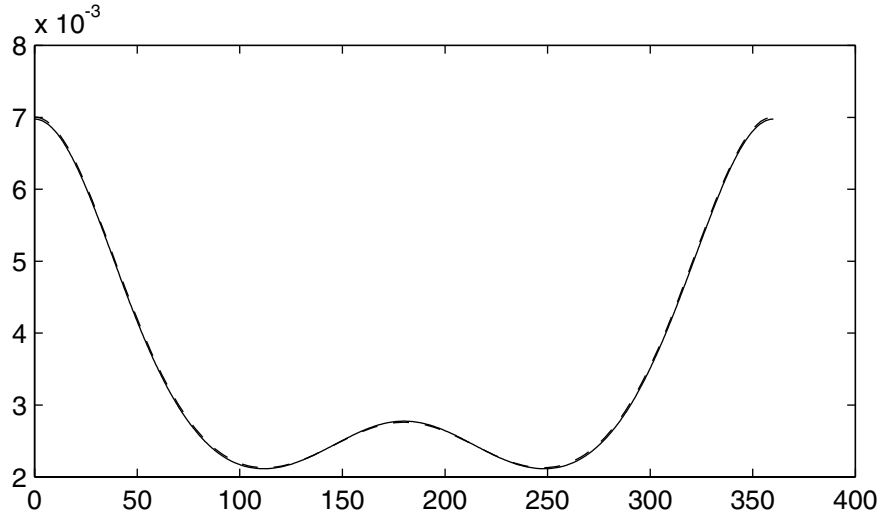

Figure 3: The normalized differential scattering cross section for a prolate spheroid with half-axes $ka = 1$ and $kb = 2$ and with relative permittivity $\epsilon = 1.5$ plotted as a function of the angle θ_p between the z-axis and radius vector in the xz-plane. The symmetry axis of the spheroid is the $x-$axis and the incident plane wave is $\boldsymbol{E}^i(\boldsymbol{r}) = E_0 e^{ikz}\hat{y}$. The solid curve is obtained by the present method and the dashed curve is the correct cross section obtained by the T-matrix method. In this graph $l_{\max} = 6$, $m_{\max} = 4$, and 256 integration points were used in the θ-integrals in Eq. (6.2). Equation (4.14) was solved numerically from a sphere with radius $kr = 0.1$ out to $kr = 2$ using the trapezoidal rule with 256 steps.

The solid curve is obtained by the present method and the dashed curve is obtained by the null-field approach using the program presented in [1]. Since Eq. (4.14) cannot be solved from $r = 0$ a small sphere with radius $kr = 0.1$ and $\epsilon = 1$ was placed at the center of the spheroid, and Eq. (4.14) was solved numerically from $kr = 0.1$ to $kr = 2$. The present method, and also the method in [6], are alternative methods to the null-field approach that was used in [10] and [1] to obtain the T-matrix. In the null-field approach, the T-matrix is obtained from a surface integral representation of the fields and an expansion of the surface fields in spherical harmonics, or regular spherical vector waves. The advantage with the null-field approach is that it is a numerically fast method, especially for spheroids, and it can handle perfectly conducting surfaces. The advantage with the propagator and the imbedding methods is that they can handle inhomogeneous dielectric bodies and that the fields can be computed everywhere.

7 Energy conservation and reciprocity

Energy conservation leads to well-known relations for the transition matrices, cf. e.g. [10]. If the shell $a < r < b$ is source free and lossless Gauss theorem gives

$$\mathrm{Re}\int_{S_b}(\boldsymbol{E}\times\boldsymbol{H}^*)\cdot\hat{r}dS = \mathrm{Re}\int_{S_a}(\boldsymbol{E}\times\boldsymbol{H}^*)\cdot\hat{r}dS$$

where S_a and S_b are the spheres with radii a and b, respectively. If there are sources in both of the regions $r < a_s$ and $r > b_s$ then

$$\begin{aligned}\mathrm{Re}\int_{S_b}&(\boldsymbol{E}^s\times\boldsymbol{H}^{s*}+\boldsymbol{E}^s\times\boldsymbol{H}^{out*}+\boldsymbol{E}^{out}\times\boldsymbol{H}^{s*})\cdot\hat{r}dS\\ &= \mathrm{Re}\int_{S_a}(\boldsymbol{E}^{in}\times\boldsymbol{H}^{in*}+\boldsymbol{E}^{in}\times\boldsymbol{H}^{r*}+\boldsymbol{E}^{r}\times\boldsymbol{H}^{in*})\cdot\hat{r}dS\end{aligned}$$

The induction law

$$\boldsymbol{H} = -\frac{i}{\omega\mu_0}\nabla\times\boldsymbol{E}$$

and the expansions of the electric fields $\boldsymbol{E}^{in}$, $\boldsymbol{E}^{out}(\boldsymbol{r})$, $\boldsymbol{E}^{r}$ and $\boldsymbol{E}^{s}$ given in Eqs. (4.3)–(4.6) lead to the following energy relation

$$\sum_{\tau n}|f_{\tau n}|^2+\sum_{\tau n}\mathrm{Re}\{a^{out}_{\tau n}f^*_{\tau n}\} = \sum_{\tau n}|a^{in}_{\tau n}|^2+\sum_{\tau n}\mathrm{Re}\{a^{in}_{\tau n}b^*_{\tau n}\}$$

By first letting $a^{in}_{\tau n}$ be zero and then $a^{out}_{\tau n}$ be zero it is seen from Eq. (5.7) that

$$\begin{aligned}T^\dagger T &= -\mathrm{Re}\{T\}\\ Q^{-1\dagger}Q^{-1} &= I+\mathrm{Re}\{R\}\end{aligned}$$

where † denotes the Hermite conjugate. These energy relations are used as tests of convergence in the numerical calculations. It is important to remember that it is a necessary condition, but not a sufficient one, that the relations are satisfied with a large number of digits.

The reciprocity relations for the transition matrices are also well-known. If $(\boldsymbol{E}^a,\boldsymbol{H}^a)$ and $(\boldsymbol{E}^b,\boldsymbol{H}^b)$ are two different fields that are source free inside a closed surface S then it follows from Gauss theorem that

$$\oint_S(\boldsymbol{E}^a\times\boldsymbol{H}^b-\boldsymbol{E}^b\times\boldsymbol{H}^a)\cdot d\boldsymbol{S} = 0$$

Let S consist of the spherical surfaces $r = a$ and $r = b$. By first letting both fields have sources in $r > b$, and then both fields have sources in $r < a$, and finally one of the fields have sources in $r < a$ and the other in $r > b$, the symmetries $T = T^t$, $R = R^t$, and $Q^{-1} = \left(\tilde{Q}^{-1}\right)^t$ are obtained.

8 Conclusions

Scattering from large objects is numerically difficult, unless high frequency approximations are used. In this paper it is shown that for a source inside an inhomogeneous spherical shell one can determine the scattered field for very large shells by a propagator method. The method is, for these particular problems, superior to purely numerical methods such as FEM, MoM, and FDTD. The method will be further developed in future work and it will be applied to radome problems. When the layers are homogeneous all matrices are diagonal in the n index, that leads to major analytical and numerical simplifications. This case is examined in a current project.

References

[1] P. W. Barber and S. C. Hill. *Light Scattering by Particles: Computational Methods*. World Scientific Publisher, Singapore, 1990.

[2] A. Boström, G. Kristensson, and S. Ström. Introduction to integral representations and integral equations for time-harmonic acoustic, electromagnetic and elastodynamic wave fields. In V. V. Varadan, A. Lakhtakia, and V. K. Varadan, editors, *Field Representations and Introduction to Scattering*, Acoustic, Electromagnetic and Elastic Wave Scattering, chapter 2, pages 37–141. Elsevier Science Publishers, Amsterdam, 1991.

[3] A. Boström and P. Olsson. Transmission and reflection of electromagnetic waves by an obstacle inside a waveguide. *Appl. Phys.*, **52**(3), 1187–1196, 1981.

[4] J. M. Jarem. Rigorus coupled-wave-theory analysis of dipole scattering from a three-dimensional, inhomogeneous, spherical dielectric, and permeable system. *IEEE Trans. Microwave Theory Tech.*, **45**, 1193–1203, 1997.

[5] J. M. Jarem. A rigorus coupled-wave-theory analysis and crossed-diffraction grating analysis of radiation and scattering from three-dimensional inhomogenous objects. *IEEE Trans. Antennas Propagat.*, **46**, 740–741, 1998.

[6] B. R. Johnson. Invariant imbedding T-matrix approach to electromagnetic scattering. *Appl. Opt.*, **27**, 4861–4873, 1988.

[7] A. Karlsson and G. Kristensson. Electromagnetic scattering from subteranean obstacles in a stratified ground. *Radio Sci.*, **18**(3), 345–356, 1983.

[8] B. Peterson and S. Ström. T-matrix for electromagnetic scattering from an arbitrary number of scatterers and representations of E(3). *Phys. Rev. D*, **8**, 3661–3678, 1973.

[9] J. A. Stratton. *Electromagnetic Theory*. McGraw-Hill, New York, 1941.

[10] P. C. Waterman. Symmetry, unitarity, and geometry in electromagnetic scattering. *Phys. Rev. D*, **3**(4), 825–839, 1971.

[11] W. Zheng and S. Ström. The null field approach to electromagnetic scattering from composite objects:the case of concavo-convex constituents. *IEEE Trans. Antennas Propagat.*, **37**, 373–383, 1989.